J. Mt. Sci. (2024) 21(9): 3108-3122 e-mail: jms@imde.ac.cn http://jms.imde.ac.cn
https://doi.org/10.1007/s11629-024-8645-5

Original Article

Prediction of the undrained shear strength of remolded soil with non-linear regression, fuzzy logic, and artificial neural network

YÜNKÜL Kaan[1*] https://orcid.org/0000-0003-1264-237X; e-mail: kaan.yunkul@gop.edu.tr

KARAÇOR Fatih[2] https://orcid.org/0000-0003-1201-7857; e-mail: fatihkaracor@gmail.com

GÜRBÜZ Ayhan[3] https://orcid.org/0000-0002-0459-7129; e-mail: agurbuz@gazi.edu.tr

BUDAK Tahsin Ömür[4] https://orcid.org/0000-0002-0265-1240; e-mail: omurbudakk@gmail.com

**Corresponding author*

1 Department of Civil Engineering, Faculty of Engineering and Architecture, Tokat Gaziosmanpaşa University, Tokat 60100, Türkiye

2 Department of Civil Engineering, Faculty of Engineering and Architecture, Kafkas University, Kars 36000, Türkiye

3 Department of Civil Engineering, Faculty of Engineering, Gazi University, Ankara 06570, Türkiye

4 Ministry of Youth and Sports, Ankara 06090, Türkiye

Citation: Yünkül K, Karaçor F, Gürbüz A, et al. (2024) Prediction of the undrained shear strength of remolded soil with non-linear regression, fuzzy logic, and artificial neural network. Journal of Mountain Science 21(9). https://doi.org/10.1007/s11629-024-8645-5

© Science Press, Institute of Mountain Hazards and Environment, CAS and Springer-Verlag GmbH Germany, part of Springer Nature 2024

Abstract: This study aims to predict the undrained shear strength of remolded soil samples using non-linear regression analyses, fuzzy logic, and artificial neural network modeling. A total of 1306 undrained shear strength results from 230 different remolded soil test settings reported in 21 publications were collected, utilizing six different measurement devices. Although water content, plastic limit, and liquid limit were used as input parameters for fuzzy logic and artificial neural network modeling, liquidity index or water content ratio was considered as an input parameter for non-linear regression analyses. In non-linear regression analyses, 12 different regression equations were derived for the prediction of undrained shear strength of remolded soil. Feed-Forward backpropagation and the TANSIG transfer function were used for artificial neural network modeling, while the Mamdani inference system was preferred with trapezoidal and triangular membership functions for fuzzy logic modeling. The experimental results of 914 tests were used for training of the artificial neural network models, 196 for validation and 196 for testing. It was observed that the accuracy of the artificial neural network and fuzzy logic modeling was higher than that of the non-linear regression analyses. Furthermore, a simple and reliable regression equation was proposed for assessments of undrained shear strength values with higher coefficients of determination.

Keywords: Undrained shear strength; Liquidity index; Water content ratio; Non-linear regression; Artificial neural networks; Fuzzy logic

Received: 24-Jan-2024
1st Revision: 07-May-2024
2nd Revision: 04-Jun-2024
Accepted: 15-Jun-2024

1 Introduction

Soil is traditionally classified as cohesive and cohesionless. Soil particles between 2 μm and 75 μm are defined as silt while grain sizes smaller than 2 μm are defined as clay fraction (ASTM D7928-17). Generally; soil particles larger than 75 μm exhibit

cohesionless behavior while silt and clay fraction show cohesive behavior (Mitchell and Soga 2005). Cohesive soil particles tend to hold moisture due to huge surface area and chemo-mechanical behavior. Water plays an important role in the swelling, compaction, consolidation, sensitivity, pore water pressure and stress-strain etc. behavior of cohesive soils. Hence, the relationship between cohesive soils and water has been investigated intensively by researchers for years.

The undrained shear strength (C_u) of the soil is an important design parameter in geotechnical and transportation engineering. Designs of shallow and deep foundation, pavement, stability of embankments, dams, offshore structures, retaining wall and excavation in cohesive soils depend on C_u which is function of water, soil type and measurement methods (Gürbüz and Dinçergök 2009; Kayabalı and Tüfenkçi 2010; Karakan et al. 2020; Budak et al. 2022). The determination of the undrained shear strength of the soil is a noteworthy, time consuming and costly process and it requires faster loading for simulation of undrained condition in the field. Designers in geotechnical engineering often prefer to use the undrained shear strength of remolded or poor-quality soil as the lower bound. This approach might yield a reliable design and minimize unpredictable soil failures, compared to using the undrained shear strength of undisturbed soil deposits.

Undrained shear strength of the soil decreases with an increase in water content (w) which is defined as the ratio of mass of moisture in the soil to the mass of dry soil particles. Undrained shear strength of the soil decreases with an increase in water content, although empirical equations with a high coefficient of determination (R^2) between water content and undrained shear strength of the remolded soil have not been obtained by researchers since undrained shear strength is a parameter of the Atterberg consistency limits, which are the plastic and liquid limits (Ullah et al. 2017; Budak et al. 2022). Therefore, a correlation of the undrained shear strength of the soil with liquidity index (LI) (Eq. (1)) or water content ratio (WCR) (Eq. (2)) have been used to predict undrained shear strength of the remolded soil. Firstly, Skempton and Northey (1952) observed the relationship between liquidity index and undrained shear strength of remolded soil; however, researchers did not propose an empirical equation. Wroth and Wood (1978) investigated the undrained shear strength of remolded soil data reported by Skempton and Northey (1952) and observed relationship between liquidity index and the undrained shear strength and proposed an equation for remolded soil. Additionally, the relationship between undrained shear strength of remolded soil and liquidity index was approximately same for all types of cohesive soils since the sensitivity degrees of the remolded soils were close to 1 (Mitchell and Soga 2005). An alternative equation, exhibiting convex curvature, based on power law was recommended by Locat and Demers (1988) for high liquidity index (1.5<LI<6). Federico (1983) found exponential relationship between undrained shear strength and water content ratio. Nowadays several empirical correlations, which are based on exponential, power and logarithmic laws, are recommended to assess the undrained shear strength of the remolded soil. Recommended correlations between undrained shear strength of the remolded soil and LI or WCR in the literature are summarized in Table 1. Moreover, Kuriakose et al. (2017) claimed that in the case of estimating the undrained shear strength parameter of soils by using water content ratio, higher coefficient of determination (R^2) are obtained while lower values are obtained in the case of using liquidity index.

$$\mathrm{LI} = \frac{w-\mathrm{PL}}{\mathrm{LL}-\mathrm{PL}} \quad (1)$$

$$\mathrm{WCR} = \frac{w}{\mathrm{LL}} \quad (2)$$

where, PL is plastic limit which is defined as the minimum water content of the soil at which soil is deformed plastically (in-recoverable deformation) without failure, LL is liquid limit which is defined as the minimum water content of the soil at which the soil behaves like a viscous fluid or in other words, it is the boundary limit water content value where the shear strength of soil is approximately zero.

Skempton and Northey (1952) observed that the ratio of C_u at liquid limit to C_u at plastic limit is approximately 1/100. The literature review report examined by Shimobe and Spagnoli (2020) shows that the range this ratio varies from 1/360 to 1/13. Yılmaz et al. (2019) reported that the effect of the height-to-diameter ratio of the specimen on the undrained shear strength is insignificant when LI > 0. Karakan et al. (2020) prepared clay-sand mixture of two different types of clays (kaolin and calcium-montmorillonite) at a given different water content and observed that the undrained shear strengths of calcium-montmorillonite-sand mixtures were higher than kaolin-sand mixtures at the same liquidity index values. Spagnoli et al. (2018) stated that the type of clay

Table 1 Summary of relationships between undrained shear strength of remolded soil and liquidity index (LI) or water content ratio (WCR) recommended by the researchers

References	Rela.	Empirical equation	Remarks	Equation rules
Wroth and Wood (1978)	LI	$C_u = 170e^{-4.6LI}$	NA	$C_u = a \cdot e^{b \cdot LI}$
Whyte (1982)		$C_u = 1.6e^{[4.23(1-LI)]}$		
Hirata et al. (1990)		$C_u = 100e^{(-3.361LI+0.376)}$		
Koumoto and Houlsby (2001)		$C_u = e^{[(1.07-LI)/0.217]}$		
Yang et al. (2006)		$C_u = 159.6e^{-3.97LI}$		
Vinod et al. (2013)		$C_u = 161.31e^{-3.33LI}$ (*) $C_u = 184.45e^{-1.087LI}$ (**)	*: $0 < LI < 1$ **: $LI < 0$	
Ullah et al. (2017)		$C_u = 47.93e^{-2.408LI}$	NA	
Yasun (2018)		$C_u = 109.05e^{-2.99LI}$ (*) $C_u = 92.31e^{-1.88LI}$ (**)	*: pocket penetrometer test; **: unconfined compression test	
Yılmaz et al. (2019)		$C_u = 94.28e^{-5.261LI}$(*)	$1.3<H/D<2.9$	
Karakan et al. (2020)		$C_u = 210.506e^{-4.516LI}$ (*) $C_u = 119.621e^{-4.533LI}$ (**)	*: for montmorillonite mixture; **: for kaolin mixture	
Locat and Demers (1988)		$C_u = \left(\frac{1.167}{LI}\right)^{2.44}$	$1.5 < LI < 6.0$	$C_u = a \cdot LI^b$
Terzaghi et al. (1996)		$C_u = 2LI^{-2.8}$	NA	
Leroueil et al. (1983)		$C_u = \frac{1}{(LI-0.21)^2}$	$0.5 < LI < 2.5$	$C_u = \frac{1}{(LI-x)^a}$
Shimobe (2000)		$C_u = 98S_t e^{\left[\frac{\ln\left(\frac{0.4755}{LI+0.5012(1-LI)}\right)}{0.19}\right]}$	NA	$C_u = \frac{a}{LI + b(1-LI)} - x$
Koumoto and Houlsby (2001)		$C_u = e^{\frac{1.070-\ln(LI)}{0.217}}$	NA	$C_u = e^{\frac{a+\ln(LI)}{b}}$
Karakan et al. (2020)		$C_u = e^{\frac{1,1844-\ln(LI)}{0,214}}$ (*) $C_u = e^{\frac{1,055-\ln(LI)}{0,2206}}$ (**)	*: for montmorillonite mixture **: for kaolin mixture	
Kayabalı et al. (2015)		$C_u = 96 \times 0.187^{LI}$	NA	$C_u = a \cdot (b)^{LI}$
Chacko and Jacob (2018)		$C_u = -127.19LI + 117.4$	NA	$C_u = a \cdot LI + b$
Vardanega and Haigh (2014)		$C_u = e^{-3.534LI+4.063}$	NA	$C_u = e^{a \cdot LI+b}$
Kuriakose et al. (2017)		$C_u = 10^{-1.486LI+1.618}$		
Budak et al. (2022)		$C_u = e^{-5.30LI+5.27}$ (*) for CH $C_u = e^{-4.80LI+5.36}$ (*) for CL $C_u = e^{-4.37LI+4.70}$ (**) for CH $C_u = e^{-3.76LI+4.82}$ (**) for CL $C_u = e^{-5.92LI+4.70}$ (***) for CH $C_u = e^{-4.20LI+4.57}$ (***) for CL $C_u = e^{-4.80LI+4.83}$ (****) for CH $C_u = e^{-3.47LI+4.87}$ (****) for CL $C_u = e^{-4.43LI+4.87}$ (*****) for CH $C_u = e^{-3.96LI+4.82}$ (*****) for CL	*: FC **: VS ***: UC ****: UU *****: PP	
Federico (1983)	WCR	$C_u = e^{[5.25(1.161-WCR)]}$	NA	$C_u = a \cdot e^{(b \cdot WCR)}$
Lee (2004)		$C_u = 182.93e^{-2.3714WCR}$		
Spagnoli and Feinendegen (2017)		$C_u = 597.82e^{-5.131WCR}$		
Hong et al. (2003)		$C_u = 1.40WCR^{-4.5}$	NA	$C_u = a \cdot (WCR)^b$
Kang et al. (2017)		$C_u = 1.71WCR^{-4.1}$		
Sharma and Sridharan (2018)		$C_u = 0.36WCR^{-1}$		
Trauner et al. (2005)		$C_u = 10^{\frac{1.162-WCR}{0.438}}$	NA	$C_u = 10^{\left(\frac{WCR-a}{b}\right)}$
Vardanega and Haigh (2014)		$C_u = 10^{2.72-2.585WCR}$	NA	$C_u = 10^{(a+b \cdot WCR)}$

Notes: St: Sensitivity ratio; a, b and x, constant parameters; a and b are different numbers for upper bound, lower bound and suggestion equation. x is always same constant number and is not changed for upper bound, lower bound and suggestion equation. Rela.: Undrained shear strength relationship; FC: Fall cone test; PP: Pocket penetrometer test; UC: Unconfined compression test; UU: Unconsolidated-undrained test CH: High plasticity clay; CL: Low plasticity clay; H/D: height-to-diameter ratio of specimen; NA: Not available.

mineral significantly influences the relationship between undrained shear strength and liquidity index. Furthermore, Wood (1990) recommended an equation which was a function of the clay minerals. Budak et al. (2022) conducted an investigation into the effects of different measurement devices on the undrained shear strength of remolded soil by utilizing various tests, including the pocket penetrometer test, fall cone test, shear vane test, unconfined compression test, and unconsolidated-undrained test, at different water content ratios and reported that type of measurement device significantly influenced the values of the undrained shear strength. Similar results have been reported by Sharma and Bora (2003), Tanaka et al. (2012), Kayabalı et al. (2015) and Yasun (2018).

The determination of the undrained shear strength (C_u) of remolded soils is a laborious, costly, time-consuming, and error-prone process that is nevertheless an important soil parameter used in geotechnical structures. Thus, in this study, a total of 1306 results from 230 different remolded soil test settings reported in the literature were collected to predict the undrained shear strength of remolded soils using non-linear regression analyses, artificial neural networks, and fuzzy logic methods. All analyses (NLR, FL and ANN) were executed and developed on a computer equipped with an AMD Ryzen 5 processor clocked at 3.10 GHz, boasting 32 GB of RAM, and running on a Windows 10 64-bit operating system. NLR analyses were conducted using Statistical Package for the Social Sciences 22 (SPSS 22) to derive empirical equations for determination of the C_u values using liquidity index (LI) and water content ratio (WCR). Moreover, fuzzy logic (FL) was utilized to forecast C_u values for remolded soil. Mamdani inference system was preferred in fuzzy logic system. Water content (w), plastic limit (PL), and liquid limit (LL) were used as input values while C_u values were selected as output parameter. Additionally, artificial neural networks (ANNs) were created in order to assess the C_u values from liquid limit or plastic limit or water content values belonging to numerous soil samples in the literature. ANN modelling was performed using MATLAB R2022b with Neural Net Fitting application. Network structure used in this study was Feed-Forward and training ANN model was also performed by using the Levenberg- Marquardt back-propagation algorithm. MAPE, NSE, NRMSE and R^2 values which are obtained by non-linear regression analyses, fuzzy logic and artificial neuron network were compared.

2 Datasets Measured

1306 data from 21 publications in the present study were collected and analyzed to predict undrained shear strength of remolded soil with NLR analysis, FL and ANN modelling for soil types of high plasticity clay (CH), low plasticity clay (CL), high plasticity silt (MH) and low plasticity silt (ML). The collected values of PI and LL of 230 different remolded soils are presented on the plasticity chart in Fig. 1. The effects of the type of clay minerals (kaolin, illite, montmorillonite etc.), soil groups and test methods were not taken into account in this study due to the lack of the data.

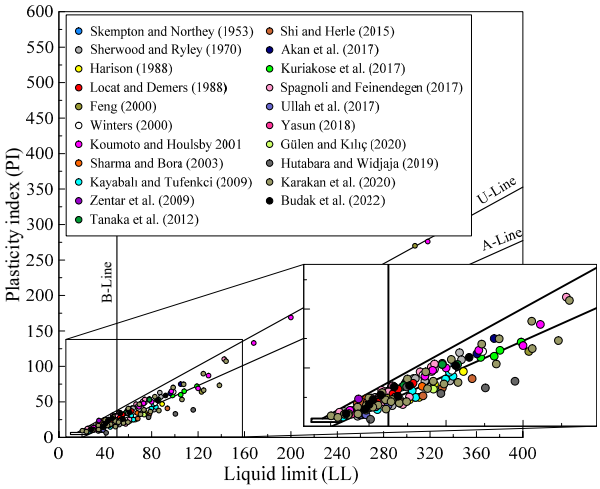


Fig. 1 Used data points on the plasticity chart.

Undrained shear strengths of the remolded soil samples were determined by researchers while using unconfined compression (UC) test, unconsolidated-undrained (UU) test, vane shear (VS) test, pocket penetrometer (PP) test, fall cone (FC) test and viscometer (V). Similar to the previous studies, only plastic and liquid state of the soil were investigated in this study. Semi-solid or solid state samples were not included. In addition, test results with undrained shear strength less than 0.1 kPa were not included in this study due to the possibility of measurement errors. The range of undrained shear strengths, plastic limits, liquid limits, water contents, liquidity indexes, water content ratios, test methods and soil types are presented in Table 2. Additionally, the average and median values of data (w, PL, LL, LI, WCR, C_u) sourced from the literature, as detailed in Table 2, are summarized in Table 3.

Table 2 Properties of the remolded soils used in this study

References	C_u (kPa)	PL	LL	w (%)	LI	WCR	Soil type	Test method	Remarks
Skempton and Northey (1952)	0.42-143.25	16-32	30-84	16-109	0-1.45	0.36-1.19	CH-CL	VS	NA
Sherwood and Ryley (1970)	0.81-4.75	14-34	17-88	21-88	0.62-1.41	0.80-1.71	CH-CL-MH-ML	FC	C_u values were obtained by Hansbo (1957) equation and cone factor was taken as 0.83 recommended by Zreik et al. (1995)
Harison (1988)	1.08-21.76	38-42	61-89	46-108	0.33-1.19	0.73-1.06	MH	FC	
Locat and Demers (1988)	0.11-1.35	14-26	27-63	35-194	1.08-3.00	0.84-2.00	CH-CL	V	NA
Feng (2000)	1.01-64	19-59	42-307	22-400	0.07-1.34	0.18-1.30	CH-CL-MH	FC	C_u values were obtained by Hansbo (1957) equation and cone factor was taken as 0.83 recommended by Zreik et al. (1995)
Winters (2000)	4-34	24-35	68-99	61-88	0.54-0.95	0.73-0.97	CH	VS	NA
Sharma and Bora (2003)	0.36-246	14-33	38-67	14-88	0-1.62	0.37-1.31	CH-CL	FC-UC	
Koumoto and Houlsby (2001)	0.61-130.3	16-51	30-318	18-397	0-1.46	0.13-1.25	CH-CL-MH	FC	
Kayabalı and Tüfenkçi (2010)	1.2-530	18-47	26-84	18-84	0-1.00	0.41-1.00	CH-CL-MH-ML	VS	
Zentar et al. (2009)	1.01-2.68	24	37	24-43	0.32-1.75	1.00-1.23	CL	VS	
Tanaka et al. (2012)	0.41-19.50	22-33	58-86	40-127	0.47-1.77	0.67-1.48	CH	FC	
Shi and Herle (2015)	0.71-2.91	14-53	34-94	30-95	0.72-1.43	0.85-1.17	CL-MH	FC	
Akan et al. (2017)	83.85-201.63	30-34	96-105	24-48	0.02-0.22	0.39-0.50	CH	UC	
Kuriakose et al. (2017)	1.53-33.90	39-47	98-119	51-92	0.11-1.00	0.49-1.00	CH-MH	VS	
Spagnoli and Feinendegen (2017)	3.3-65.5	12-39	25-143	16-52	0.15-0.98	0.34-0.99	CH-CL-MH	VS	
Ullah et al. (2017)	2.87-56.40	22-32	35-50	22-50	0-1.00	0.62-1.00	CL-ML	VS	
Yasun (2018)	17-232	20	31	18-27	0.02-0.65	0.47-0.88	CL	PP-UC	
Gülen and Kılıç (2020)	1.48-28.44	18-41	31-73	23-78	0.14-1.28	0.66-1.10	CH-CL-MH	VS	
Hutabarat and Widjaja (2020)	1.74-187	24-77	40-116	26-103	0.06-1.18	0.56-1.08	CH-CL-MH-ML	FC	
Karakan et al. (2020)	0.40-66.26	10-65	20-144	12-185	0-2.12	0.48-1.44	CH-CL-MH-ML	FC	
Budak et al. (2022)	0.43-480	19-33	28-92	11-95	0-1.04	0.36-1.02	CH-CL	FC-PP-UU-UC-VS	UU tests under the confining pressure of 50, 100 and 200 kPa were performed

Note: FC: Fall cone test; PP: Pocket penetrometer test; UC: Unconfined compression test; UU: Unconsolidated-undrained test; V: Viscometer; VS: Vane shear test; CH: High plasticity clay; CL: Low plasticity clay; MH: High plasticity silt; ML: Low plasticity silt; NA: Not available.

3 Performance Measurement

In the present paper, Non-linear regression (NLR) analyses, fuzzy logic (FL) and artificial neural network (ANN) methods were used to predict the undrained shear strengths of the remolded soil samples. The prediction accuracy and performance of FL, ANN and NLR models needs to be evaluated. In the other words, the aim is to assess the closeness of predictions of

Table 3 Descriptive statistics of the data

Parameter	Average ± S.D.	Median (Min.-Max.)
w (%)	53.5±40.2 (%)	42.2 (11.09-400.00) (%)
PL	27.9±10.3	25 (10.9-77.1)
LL	65.0±42.5	55 (17-318)
LI	0.7±0.7	0.6 (0-6.03)
WCR	0.8±0.4	0.8 (0.14-3.69)
C_u (kPa)	37.1±65.2 (kPa)	9.6 (0.02-530.00) (kPa)

Note: S.D.: Standard deviation.

values of undrained shear strength of remolded samples from non-linear regression, fuzzy logic and artificial neural network to the real values. In this respect, three different error metrics which are mean absolute percentage error (MAPE) (Eq. (3)), Nash–Sutcliffe model efficiency (NSE) (Eq. (4)), coefficient of determination (R^2) (Eq. (5)) and normalized root mean square error (NRMSE) are utilized (Eq. (6)). These error metrics are generally used for model validation and model comparisons and model selections.

$$\text{MAPE} = \frac{1}{n}\sum_{i=1}^{n}\frac{|R_i - P_i|}{R_i} \quad (3)$$

$$\text{NSE} = 1 - \frac{\sum_{i=1}^{n}(R_i - P_i)^2}{\sum_{i=1}^{n}(R_i - \text{mean of } R)^2} \quad (4)$$

$$R^2 = 1 - \frac{\sum_{i=1}^{n}(R_i - P_i)}{\sum_{i=1}^{n}(R_i - \overline{R_i})} \quad (5)$$

$$\text{NRMSE} = \frac{\sqrt{\frac{1}{n}\sum_{i=1}^{n}(R_i - P_i)^2}}{\text{mean of } R} \quad (6)$$

where, R_i is real output parameter, P_i is predicted output parameter, $\overline{R_i}$ is average value of real output parameter n is total sample.

The coefficient of determination (R^2) values range from 0 to 1. The strong relationship is observed between real and predicted output when the value of R^2 is close to 1. Furthermore, a lower value of MAPE and NRMSE indicates higher accuracy of the model, whereas a higher value of NSE also signifies greater accuracy.

4 Results and Discussions

In this study, the following limitations were imposed on the methods (NLR, FL, ANN) used to analyze and the collected data.

- Data of remolded soils were collected. The study did not incorporate undisturbed soil data obtained directly from field conditions.
- C_u values less than 0.1 kPa were not included.
- The C_u data in solid and semi-solid states with liquidity index values less than 0 are not included.
- Only C_u data obtained from fall cone, pocket penetrometer, unconfined compression, unconsolidated-undrained, viscometer, vane shear test were used.
- The soil type in the data are high plasticity clay, low plasticity clay, high plasticity silt and low plasticity silt.
- In some regression analyses, data points with liquidity index values below 0.15 were excluded.
- FL operates within the limits of a predefined set of rules established based on expert judgments.
- The data were gathered from indexed journals and extensively cited studies in the literature. It's worth noting that results might differ with a larger dataset

4.1 Non-linear regression analysis

Non-linear regression (NLR) analyses with statistical analysis software SPSS 22 were performed to develop a predictive model for C_u. Liquidity index (LI) or water content ratio (WCR) were taken as input parameters and undrained shear strength of the 1306 remolded soils from 21 publications was taken as output parameter while recommended equation rules in Table 1 were taken into considerations. Thus, 12 different non-linear regression analyses Eqs.(7)-(18) with upper and lower limits having of 95% confidence limit were obtained with SPSS 22. The results of the obtained non-linear regression analyses are summarized in Table 4.

A noteworthy relationship via of Eq. (9) with (R^2=0.911) between liquidity index and undrained shear strength of remolded soil was observed. The relationship among undrained shear strength-liquidity index and undrained shear strength-water content ratio from the collected data were compared with the results of Eqs. (9), (11), (14), (17), (18) that yield to higher coefficient of determination values (R^2) and presented in Fig. 2a and 2b, respectively. The liquidity index value of 0.15 is the boundary condition for Eq. (9) and Eq. (11), so it is not recommended to use these equations when the liquidity index values are lower than 0.15.

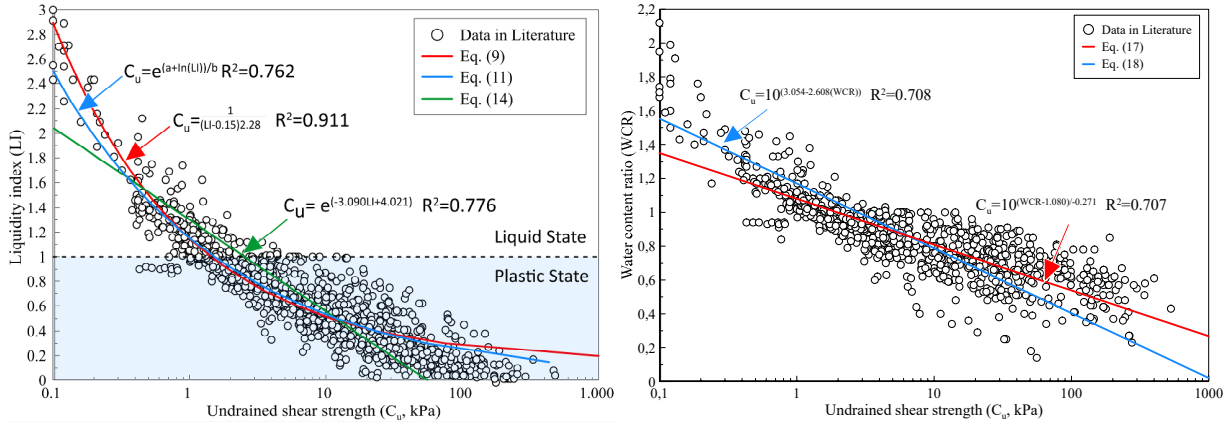
4.2 Fuzzy Logic (FL) analyses

The fuzzy set theory was firstly introduced by Zadeh (1965). Traditionally binary values (0-1) are preferred in fuzzy logic (FL) although intermediate values can be used. The data could take values between

Table 4 Recommended empirical equations derived in present study

Equation number	Equation rules	Remarks	R^2	Lower bound		Equation		Upper bound	
				a	b	a	b	a	b
7	$C_u = a \cdot e^{b*LI}$	NA	0.58	110.775	-4.346	119.283	-4.020	127.790	-3.693
8	$C_u = a \cdot LI^b$		0.497	9.377	-0.810	10.507	-0.767	11.637	-0.724
9	$C_u = \frac{1}{(LI-x)^a}$	$LI > 0.15$ $x = 0.15$	0.911	2.258	-	2.280	-	2.303	-
10	$C_u = \frac{a}{LI + b(1-LI)} - x$	$x = 11.530$	0.455	14.890	0.476	13.955	0.030	15.826	0.086
11	$C_u = e^{\left(\frac{a+\ln(LI)}{b}\right)}$	$LI > 0.15$	0.762	-0.117	-0.348	-0.143	-0.336	-0.170	-0.323
12	$C_u = a \cdot (b)^{LI}$	NA	0.580	110.766	0.012	119.283	0.018	127.800	0.024
13	$C_u = a \cdot LI + b$		0.306	-39.958	41.354	-36.418	44.474	-32.878	47.594
14	$C_u = e^{a \cdot LI+b}$		0.776	-3.197	3.927	-3.090	4.021	-2.982	4.116
15	$C_u = a \cdot e^{(b*WCR)}$		0.322	334.762	-3.738	407.126	-3.421	479.490	-3.104
16	$C_u = a \cdot (WCR)^b$		0.215	18.135	-1.521	20.728	-1.384	23.320	-1.247
17	$C_u = 10^{\frac{WCR-a}{b}}$		0.707	1.067	-0.260	1.080	-0.271	1.092	-0.282
18	$C_u = 10^{a+b \cdot WCR}$		0.708	2.960	-2.204	3.054	-2.608	3.147	-2.713

Note: a, b and x symbolize constant parameters. a and b are different numbers for upper bound, lower bound and suggestion equation. x is always same constant number and is not changed for upper bound, lower bound and suggestion equation. NA: not available.



(a) (b)

Fig. 2 Comparison of recommended equation with data. (a) Relationship undrained shear strength and liquidity index; (b) Relationship undrained shear strength and water content ratio.

0 and 1. Fuzzy logic consists of four main components: (1) fuzzification, (2) fuzzy rule base, (3) inference mechanism, and (4) defuzzification. The proce ssing diagram of fuzzy logic are presented in Fig. 3. Firstly, input parameters in the fuzzification stage where numerous membership functions (Gaussian, sigmoid, trapezium, triangle) used are converted to fu zzy sets. Secondly, inference mechanism investigates the degree of match among fuzzy inputs with help of the fuzzy rules that contain all conditions the users define. The resulting fuzzy set is converted to crisp values in the defuzzification stage. The fuzzy set is defined by membership function (Eq. (19)).

$$A = \{x, ; \mu_A(x)\} | \, x \in X \quad (7)$$

where, A is a fuzzy function and represented by a membership function ($\mu_A(x)$), which defines the membership degree having values of 0 to 1, in the information universe (X). The value of 0 means that $\mu_A(x)$ is not a member in fuzzy set, the value of the 1 means that $\mu_A(x)$ is a fully member in fuzzy set and the values between 0 and 1 mean that $\mu_A(x)$ is a partial

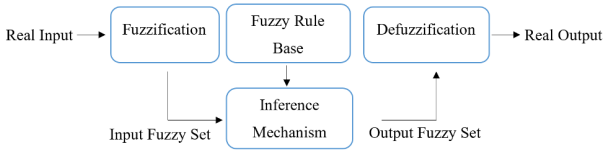


Fig. 3 Processing diagram of fuzzy logic.

member in fuzzy set.

The data used in the study is composed of three different input parameters of water content, plastic limit, liquid limit and one output parameter of undrained shear strength which was divided into five different categories and classified as very low (VL), low (L), medium (M), high (H) and very high (VH) (Fig. 4). The fuzzy logic model was created and analyzed using the MATLAB R2022b with analysis times ranging from 370.6 to 440.9 seconds. The cut-off points used for classifications are presented in Table 5. The consistency ranges recommended by Terzaghi et al. (1996) and BS5930 (2015) were taken as the basis for determining the cut-off points. The Mamdani inference system was used because interpretability of the inference system is easier than Sugeno inference system. In the presented study, triangular membership function was used for variables in L, M, and H categories while trapezoidal membership function was preferred for the variables in VL and VH categories. Additionally, the degree of the membership was normalized between 0 and 1. After creating membership function and categories for input and output, the fuzzy rules were established and presented in Table 6. The created rule list was validated by five different people who are experts in their field (minimum 10 years of experience) in a five-point Likert type (1: lowest, 5: greatest).

Table 5 Cut-off points used for variables in the fuzzy logic model

Classification	w	PL	LL	C_u
Very low (VL)	20	15	20	50
Low (L)	30	25	35	100
Medium (M)	40	35	50	150
High (H)	50	45	65	200
Very high (VH)	60	55	80	250

4.3 Artificial Neural Network (ANN) analyses

Artificial Neural Networks (ANN) have been inspired from the working mechanism and structure of human brain nervous system. The aim of the ANN is to replicate the way of learning of human brain through mathematical algorithms using connected the artificial neurons. ANNs are nowadays preferred to solve complex problems including speech, identification,

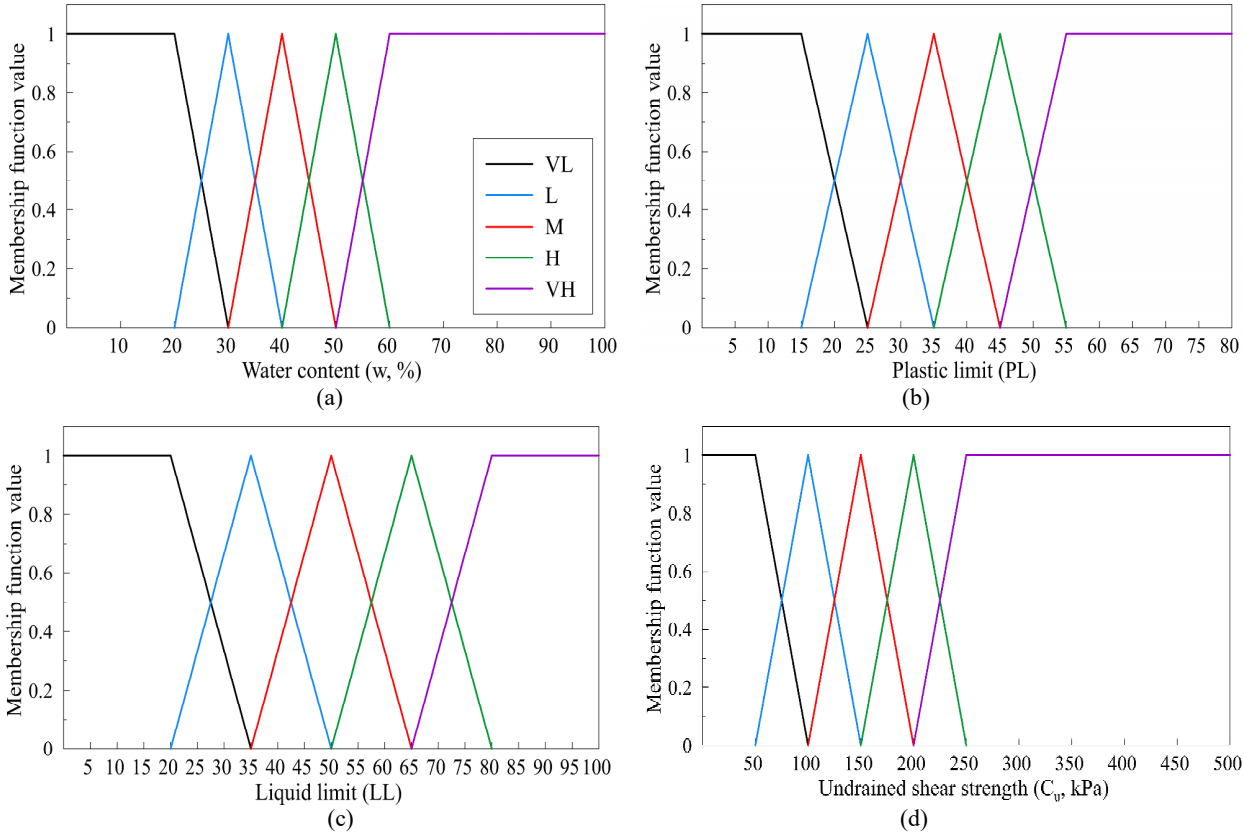


Fig. 4 Membership functions of input and variables. (a) Water content; (b) Plastic limit; (c) Liquid limit; (d) Undrained shear strength.

simulation, numerical prediction, recognition. Artificial Neural Network systems can be trained through given samples and consist of sequence layers which are interconnected to each other. After ANN training, the system learns information from given samples and the new samples can be predicted. Generally, ANN systems consist of input layer, layer and output layer with number of neurons and different transfer functions (Fig. 5). The weighted sum of inputs transmits to hidden neurons and then to outputs via using an activation function. The outputs of the hidden neurons, in turn, act as inputs to the output neuron where it undergoes another transformation.

ANN performance depends on the number of input, output and hidden layers, the number of neurons in hidden layer and the transfer function. In the literature, no general ANN rules have been identified for the number of hidden layers and neurons in hidden layer. Structure of the ANN system is determined by using trial and error. In this study, MATLAB R2022b software with Neural Net Fitting application was used to train and develop ANN models for predicting undrained shear strength of remolded soils. Analysis duration of the ANN models varied between 460.1 and 483.4 seconds. The network type and the transfer function were selected as Feed-Forward backpropagation and TANSIG function, respectively. Additionally, ANN modelling was performed by Levenberg-Marquardt back-propagation algorithm. The network is built with a single hidden layer with 10 neurons (Fig. 5). Undrained shear strength was used as output parameter while water content, plastic limit and liquid limit values were used as input parameters in Fig. 5. The neural network modelling process is divided into three phases; training, validation and test phases. Training phase is preferred to train ANN model and to assess weights of the neurons. The validation phase is used to halt the learning phase and training phase due to preventing overfitting problems. Additionally, the validation phase supplies reference to estimate parameters by the output from forward propagation although training phases performs back propagation. Test phase is used to define the effectiveness of trained phase. In this study, the experimental data set is divided randomly such that 70% of samples were used for training, 15% for validation and, 15% for testing. Similar percent of training, validation and testing have been recommended by several researchers (Kalkan et al. 2009; Dehghanbanadaki et al. 2019; Moayedi and

Table 6 List of rules used in fuzzy logic

Rule number	w	PL	LL	C_u	Average expert grade (5 point Likert Scale)
1	VL	VL	VL	VH	4.8
2	VL	VL	L	H	4.2
3	VL	VL	M	H	4
4	VL	VL	H	H	3.8
5	VL	VL	VH	M	4
6	VL	L	VL	H	4.2
7	VL	L	L	M	3.8
8	VL	L	M	M	4.4
9	VL	L	H	L	4
10	L	VL	VL	VL	5
11	L	VL	L	VL	4.2
12	L	VL	M	VL	4
13	L	L	L	VL	4.4
15	L	L	M	VL	4
16	L	L	H	VL	4.2
19	M	VL	L	VL	4
20	M	VL	M	VL	3,8
21	M	L	L	VL	4.4
22	M	L	M	VL	3.6
23	H	L	M	L	4
24	H	L	H	VL	4.4
25	H	M	M	L	3.6
26	H	M	H	VL	4.2
27	H	M	VH	VL	4.6
28	VH	L	VL	VL	4.2
29	VH	L	L	VL	4.6
30	VH	L	M	VL	4.4
31	VH	L	H	VL	4.4
32	VH	L	VH	VL	4.8
33	VH	M	H	VL	3.8
34	VH	M	VH	VL	4.6
35	VH	H	VH	VL	4.4
36	VH	VH	VH	VL	5

Note: VL: Very low; L: Low; M: Medium; H: High; VH: Very high.

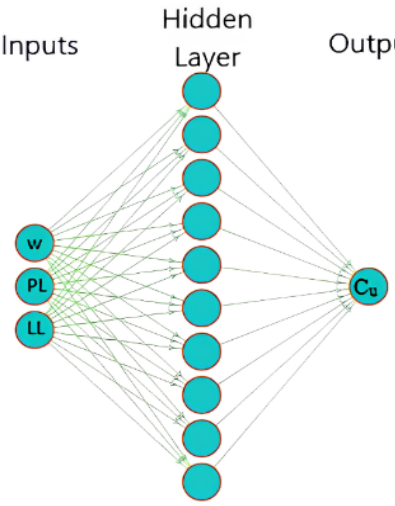


Fig. 5 Artificial Neural Network structure.

Hayati 2019; Taleb Bahmed et al. 2019; Abu-Farsakh and Mojumder 2020; Moayedi et al. 2020; Akbay Arama et al. 2021; Gökçeoğlu 2022; Lin et al. 2022).The average coefficient of correlation values (R) from ANN model were determined as 0.9761, 0.9778, 0.9663, and 0.9748 for training, validation, test and finally using complete dataset, respectively as presented in Fig. 6.

4.4 Comparing NSE, MAPE, NRMSE and R² values of test methods

The obtained NSE, MAPE, NRMSE and R^2 values for non-linear regression analyses, fuzzy logic, and artificial neuron network are presented in Table 7. Only five non-linear regression equations (Eqs.(9), (11), (14), (17), (18)) are investigated because of high R^2 performance in Table 7. The results presented in Table 6 indicate that Fuzzy logic (FL) and artificial neuron network gave more accurate results than traditional non-linear regression analyses. Similar finding has

Table 7 Comparison NSE, MAPE, and R^2 values of non-linear regression, fuzzy logic and artificial neuron network analyses

Method	MAPE (%)	NSE	NRMSE (%)	R^2
NLR Eq. (9)	14.07	0.853	12.30	0.911
NLR Eq. (11)	36.29	0.644	28.28	0.762
NLR Eq. (14)	26.04	0.709	25.68	0.776
NLR Eq. (17)	39.72	0.391	34.16	0.707
NLR Eq. (18)	39.42	0.453	31.96	0.708
FL	38.95	0.483	28.34	0.923
ANN	5.66	0.934	6.95	0.942

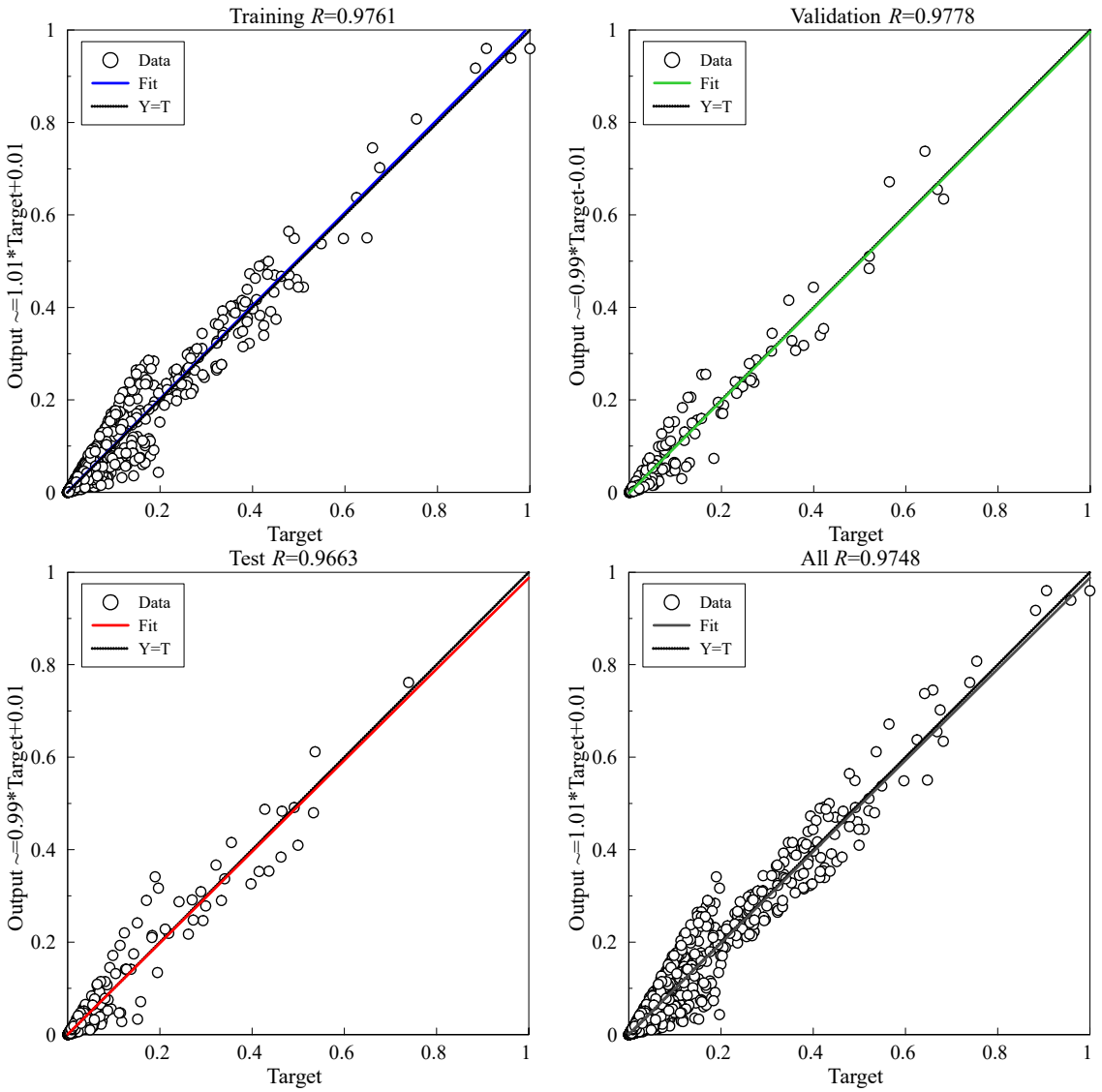


Fig. 6 R-value results of the Artificial Neural Network analysis for the training, validation, and test data.

been reported by several researchers (Işık 2009; Akan and Keskin 2019; Taleb Bahmed et al. 2019; Mbarak et al. 2020; Akbay Arama et al. 2021; Gökçeoğlu 2022; Saadat and Bayat 2022) for prediction of geotechnical engineering parameters. The best performance was observed in Eq. (9) for non-linear regression analyses. Additionally, proposed regression analyses recommend equations for geotechnical designers to predict undrained shear strength of remolded soil. It is difficult for designers to understand or interpret the results from ANN and FL and in addition, ANN and FL results are not practical to prediction of undrained shear strength of the remolded soil. Thus, designers could be able to estimate undrained shear strength of remolded soil rapidly with simple regression equations instead of complex FL and ANN.

The results of the test data used in ANN (n:196) in all models were compared with the actual results (Table 8). Kruskal Wallis H test was applied for comparison and it was statistically significant (X^2=29.465; p<0.001). Post-hoc analysis was performed to determine the groups that caused a significant difference. As a result of the analysis; Eq. (11) (34.3±5.3; 3.2) with other groups Actual (38.2±4.4; 9.2), Eq.(9) (38.0±6.8; 8.7), Eq.(14) (34.0±5.5; 8.6), Eq.(17) (28.4±6.9; 9.9), Eq.(18) (30.2±3.7; 4.4) and FL (40.4±3.5; 14.4) are statistically significantly different (p^{ac}=0,001; p^{bc}=0,002; p^{cd}=0,001; p^{ce}=0,001; p^{cf}<0,001). Additionally, similar to Eq. (18) (30.2±3.7; 4.4), Actual (38.2±4.4; 9.2), Eq. (9) (38.0±6.8; 8.7) and FL (40.4±3.5; 14.4) are statistically significantly different from other groups (p^{af}=0,002; p^{bf}<0,001; p^{fg}<0,001).

The determination was made that the data deviated from a normal distribution based on the Shapiro-Wilk test (p<0.05), as well as the kurtosis and skewness values (|Skewness and Kurtosis|> 2.5). Consequently, the Mann Whitney U-test (Table 8) was employed for pairwise group comparisons, while the Kruskall Wallis H-test (Table 9) was utilized for multigroup comparisons. For each of the tested models, the results of their own test data and the actual results were compared with the Mann Whitney U-test. As a result of the analysis, there is no statistically significant difference between the pairs (p>0.05).

The distribution of errors resulting from the applied test methods is depicted in violin density plots (Fig. 7). As depicted in Fig. 7, the errors of the values obtained from Eqs. (11), (14), (17), and (18) exhibited a significantly wide distribution. Additionally, ANN, which outperformed these equations, as well as Eq. (12) and FL models, are elaborated upon in detail.

The Taylor diagram is a commonly preferred method for displaying the accuracy of developed models or equations. In this study, the accuracy of Eqs. (9), (11), (14), (17), and (18), as well as the FL and ANN methods, is presented on the Taylor diagram in Fig. 8. Analysis of the Taylor diagram reveals that the standard deviations of the FL and ANN methods are very close to the actual result. The poorest performing

Table 8 Comparison of the results obtained from the methods for the test data used in ANN

Method	n	Mean ± S.D.	Median (Min.-Max.)	X^2	p
Actual (a)	196	38.2±4.4	9.2 (0.1-391.9)	29.465	<0.001
NLR Eq. (9) (b)	196	38.0±6.8	8.7 (0.1-473.4)		p^{ac}=0.001
NLR Eq. (11) (c)	196	34.3±5.3	3.2 (0.1-369.7)		p^{bc}=0.002
NLR Eq. (14) (d)	196	34.0±5.5	8.6 (0.1-481.9)		p^{bf}<0.001
NLR Eq. (17) (e)	196	28.4±6.9	9.9 (0.1-423.6)		p^{cd}=0.001
NLR Eq. (18) (f)	196	30.2±3.7	4.4 (0.1-374.0)		p^{ce}=0.001
FL (g)	196	40.4±3.5	14.4 (0.1-290.5)		p^{cf}<0.001
ANN (h)	196	38.0±4.5	6.9 (0.1-403.7)		p^{fg}<0.001

Table 9 Comparison of the results obtained for each model with real results

Method	n	Model Results	Actual Results	z	p
		Mean ± S.D.	Mean ± S.D.		
NLR Eq. (9)	1073	26.6±70.6	26.2±25.6	-0.219	0.827
NLR Eq. (11)	1073	33.0±70.6	26.2±25.6	-0.634	0.526
NLR Eq. (14)	1306	30.2±74.3	37.1±65.2	-0.821	0.412
NLR Eq. (17)	1306	37.8±62.5	37.1±65.2	-0.319	0.728
NLR Eq. (18)	1306	29.4±55.5	37.1±65.2	-1.646	0.100
FL	1306	41.3±51.4	37.1±65.2	-0.407	0.684
ANN	196	38.0±66.8	38.1±62.1	-0.778	0.436

Note: n: Number of the test data; S.D.: Standard deviation; z: Mann Whitney U-test; p: p value. The p-value is significant when the it is less than 0.05.

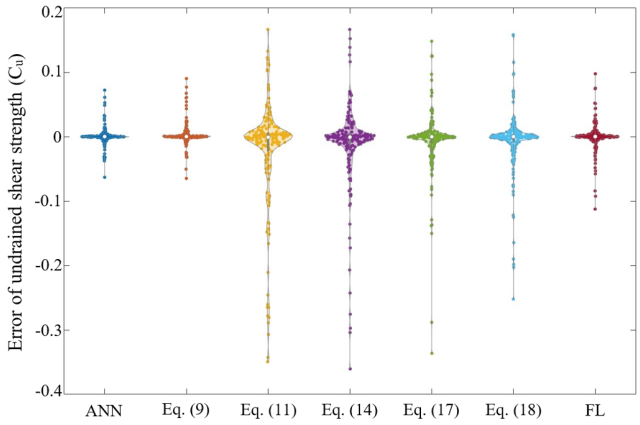


Fig. 7 Violin plots of Eqs. (9), (11), (14), (17), (18), ANN and FL.

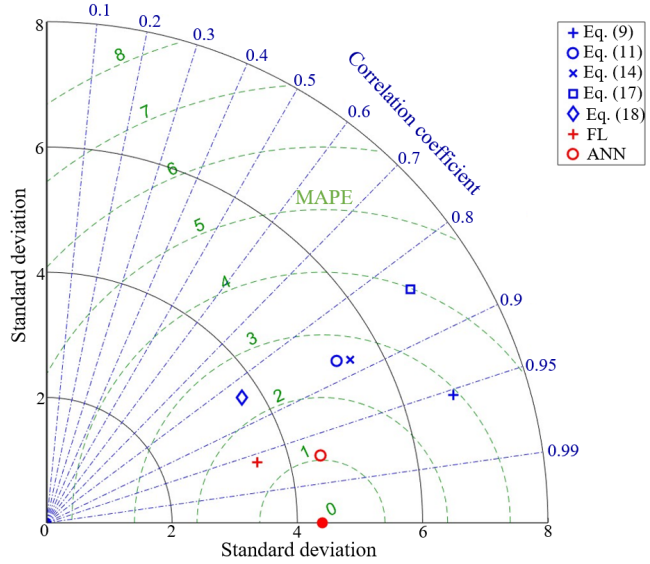


Fig. 8 Taylor diagram for evaluating the accuracy of the methods.

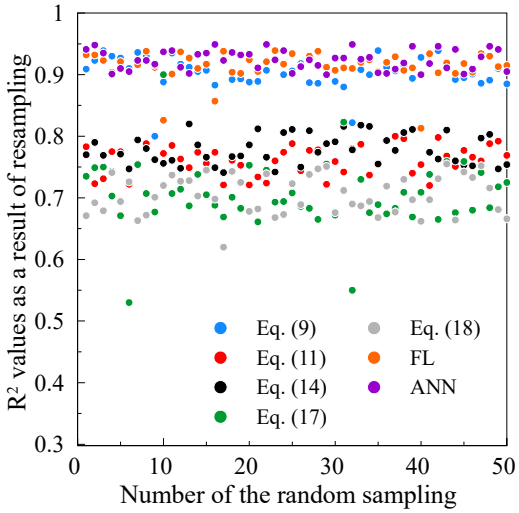


Fig. 9 R^2 values resulting from resampling of Eqs. (9), (11), (14), (17), (18), ANN and FL.

model was identified as Eq. (17), characterized by a large standard deviation and a low correlation coefficient. However, the correlation coefficients of the FL, ANN methods, and Eq. (9) with the actual results range from 0.95 to 0.99, indicating high reliability.

Reliability of the methods also investigated in this study. 80 percent of the data was selected 50 times using the random sampling method, and the R^2 values were calculated for each of these and are shown in Fig. 9. The R^2 values obtained from ANN, FL and Eq. (9) are concentrated between 0.86 and 0.95 however, it was observed that R^2 values of other models were both lower and scattered.

5 Conclusions

In this paper, non-linear regression (NLR), fuzzy logic (FL) and artificial neural network (ANN) models were developed to predict undrained shear strength (C_u) of remolded soils. Feed-Forward backpropagation, TANSIG function and, Levenberg-Marquardt back-propagation algorithm were used for ANN modelling. Mamdani inference system was preferred with trapezoidal and triangular membership function for fuzzy logic. Although liquidity index (LI) and water content ratio (WCR) were used for non-linear regression (NLR) analyses, water content (w), plastic limit (PL) and liquid limit (LL) were used for FL and ANN. For this aim, totally 1306 undrained shear strength values that are obtained from 230 different remolded soil test values were collected from the literature. Based on the results, following conclusion are presented.

- Non-linear relationship has been observed between liquidity index (LI) or water content ratio (WCR) and undrained shear strength of remolded soil although a clear relationship between water content and C_u was not observed. Additionally, there is a decrease in the undrained shear strength with the increase of LI or WCR. Five different regression equations were recommended to predict undrained shear strength of remolded soil with high R^2 values.
- A satisfactory performance was obtained from ANN and FL for prediction of

undrained shear strength of remolded soil with high coefficient of determination (R^2=0.942, 0.923), high Nash-Sutcliffe model efficient (NSE=0.934, 0.483) low mean absolute percentage error (MAPE=5.66%, 38.95%) and low normalized root mean square error (NRMSE=6.95%, 28.34%) corresponding to non-linear regression results. ANN and FL models are suitable methods for prediction of different complex behavior of remolded clay samples.

- Although the accuracy of the ANN and FL were higher than traditional regression analyses, regression analyses proposed equations for designers. In this study, proposed regression equations cause quickly prediction of the undrained shear strength depending on water content ratio or liquidity index. Thus, proposed equations should be used and developed for geotechnical or transportation engineering application and they can be used as generalized tool for guidance.
- In general, geotechnical or transportation engineering studies include human errors, insufficient measurement devices, environmental conditions and, cause underestimated designs to appear. Designers will be able to reliable design thank to recommended equations.

This study focuses on predicting the undrained shear strength of remolded soil using various soil parameters, including liquidity index, water content ratio, water content, plastic limit, and liquid limit. Semi-solid and solid state and, undrained shear strength less than 0.1 kPa were not investigated in the study. Additionally, only data for four different soil types (CL, CH, ML and MH classes) with six measurement devices (unconfined compression, shear vane, pocket penetrometer, unconsolidated undrained, fall cone, and viscometer test) were used. There remains a multitude of research avenues and deficiencies that warrant further investigation. In future research, it is imperative to investigate methods for predicting the undrained shear strength of both undisturbed and disturbed soil, as well as remolded soil in semi-solid or solid state. Also, the relationship between sensitivity ratio and undrained shear strength should be analyzed. This will contribute to fast and reliable determination of undrained shear strength of soil.

Acknowledgments

The authors would like to thank Dr. Murat Ayhan and reviewers for their help and contributions to the work presented in this paper.

Author Contribution

YÜNKÜL Kaan: Conceptualization, Investigation, Methodology, Resources, Visualization, Writing-original draft, Writing-review & editing. KARAÇOR Fatih: Data curation, Visualization, Writing-review & editing. GÜRBÜZ Ayhan: Conceptualization, Supervision, Writing-review & editing. BUDAK Tahsin Ömür: Conceptualization.

Ethics Declaration

Availability of Data/Materials: Data is available on reasonable request from the corresponding author.

Conflict of Interest: The authors declare that they have no known competing financial interests or personal relationships that could have appeared to influence the work reported in this paper.

References

Abu-Farsakh MY, Mojumder MAH (2020) Exploring artificial neural network to evaluate the undrained shear strength of soil from cone penetration test data. Transp Res Rec 2674(4):11-22. https://doi.org/10.1177/0361198120912426

Akan R, Keskin SN (2019) The effect of data size of ANFIS and MLR models on prediction of unconfined compression strength of clayey soils. SN Appl Sci 1(8):1-11. https://doi.org/10.1007/s42452-019-0883-8

Akan R, Keskin SN, Yazıcı MF (2017) The relationship between the water content and unconfined compressive strength of clayey soils. Kilis 7 December University Journal of Science and Engineering 1(2): 1-9.

Akbay Arama Z, Yücel M, Akın MS, Dalyan I (2021) A comparative study on the application of artificial intelligence networks versus regression analysis for the prediction of clay plasticity. Arab J Geosci 14(7):1-16. https://doi.org/10.1007/s12517-021-06894-x

ASTM D7928-17 (2017) Standard Test Method for Particle-Size Distribution (Gradation) of Fine-Grained Soils Using the Sedimentation (Hydrometer) Analysis. West Conshohocken, PA: ASTM International.

BS5930 (2015) Code of practice for ground investigations. British Standards Institution London.

Budak TO, Gürbüz A, Ekşioglu B (2022) Practical transitions among undrained shear strengths of remolded samples from pocket penetrometer tests and other laboratory tests. Catena 213:106148. https://doi.org/10.1016/j.catena.2022.106148

Chacko J, Jacob DS (2018) Study on strength characteristics of Kuttanad clay based on its water content and consistency limits.

Int Res J Eng Tech 5(4):3221-3225.
Dehghanbanadaki A, Sotoudeh MA, Golpazir I, et al. (2019) Prediction of geotechnical properties of treated fibrous peat by artificial neural networks. B Eng Geol Environ 78(3):1345-1358. https://doi.org/10.1007/s10064-017-1213-2
Federico A (1983) Relationships (Cu–w) and (Cu–s) for remolded clayey soils at high water content. Rivista Italiana di Geotecnica 17(1):38-41.
Feng TW (2000). Fall-cone penetration and water content relationship of clays. Geotechnique 50(2):181-187. https://doi.org/10.1680/geot.2000.50.2.181
Gökçeoğlu C (2022) Assessment of rate of penetration of a tunnel boring machine in the longest railway tunnel of Turkey. SN Appl Sci 4(1):1-12. https://doi.org/10.1007/s42452-021-04903-y
Gülen H, Kılıç M (2020) Determination of Strength and Deformation Parameters of Remolded Clays by Falling Cone and Veyn Tests. Teknik Dergi 31(3):9987-10012. https://doi.org/10.18400/tekderg.483348
Gürbüz A, Dinçergök T (2009) Long term behavior of staged construction of a dam on soft clay. Proceedings of the 17th International Conference on Soil Mechanics and Geotechnical Engineering, 5-9 October 2009, Alexandria, Egypt. pp 1915-1918.
Hansbo S (1957) New approach to the determination of the shear strength of clay by the fall-cone test. Royal Swedish Geotechnical Institute.
Harison J (1988) Using the BS cone penetrometer for the determination of the plastic limit of soils. Geotechnique 38(3):433-438. https://doi.org/10.1680/geot.1988.38.3.433
Hirata S, Yao S, Nishida K (1990) Multiple regression analysis between the mechanical and physical properties of cohesive soils. Soils Found 30(3):91-108. https://doi.org/10.3208/sandf1972.30.3_91
Hong ZS, Liu HL, Negami T (2003) Remolded undrained strength of soils. China Ocean Eng 17(1):133-142.
Hutabarat GM, Widjaja B (2020) Correlation of Undrained Shear Strength and Liquidity Index of Fine-Grained Soils in West Java, Indonesia. IOP Conference Series: Materials Science and Engineering 852. https://doi.org/10.1088/1757-899X/852/1/012011
Işık NS (2009) Estimation of swell index of fine grained soils using regression equations and artificial neural networks. Sci Res Essays 4(10):1047-1056.
Kalkan E, Akbulut S, Tortum A, Celik S (2009) Prediction of the unconfined compressive strength of compacted granular soils by using inference systems. Environ Geol 58(7):1429-1440. https://doi.org/10.1007/s00254-008-1645-x
Kang G, Tsuchida T, Tang T, Kalim T (2017) Consistency measurement of cement-treated marine clay using fall cone test and Casagrande liquid limit test. Soils Found 57(5): 802-814. https://doi.org/10.1016/j.sandf.2017.08.010
Karakan E, Shimobe S, Sezer A (2020) Effect of clay fraction and mineralogy on fall cone results of clay–sand mixtures. Eng Geol 279:105887. https://doi.org/10.1016/j.enggeo.2020.105887
Kayabalı K, Tüfenkçi OO (2010) Shear strength of remolded soils at consistency limits. Can Geotech J 47(3):259-266. https://doi.org/10.1139/T09-095
Kayabalı K, Akturk O, Fener M, et al. (2015) Revisiting the Bjerrum's correction factor: Use of the liquidity index for assessing the effect of soil plasticity on undrained shear strength. J Rock Mech Geotech 7(6):716-721. https://doi.org/10.1016/j.jrmge.2015.07.003
Koumoto T, Houlsby G (2001) Theory and practice of the fall cone test. Geotechnique 51(8):701-712. https://doi.org/10.1680/geot.2001.51.8.701
Kuriakose B, Abraham BM, Sridharan A, Jose BT (2017) Water content ratio: an effective substitute for liquidity index for prediction of shear strength of clays. Geotech Geol Eng 35(4):1577-1586. https://doi.org/10.1007/s10706-017-0193-0
Lee LT (2004) Method to rapidly assess the index properties of fine-grained dredged materials. Geotech Test J 27(5): 464-468. https://doi.org/10.1520/GTJ11812
Leroueil S, Tavenas F, Bihan JPL (1983) Propriétés caractéristiques des argiles de l'est du Canada. Can Geotech J 20(4):681-705. https://doi.org/10.1139/t83-076
Lin P, Chen X, Jiang M, et al. (2022) Mapping shear strength and compressibility of soft soils with artificial neural networks. Eng Geol 300:106585. https://doi.org/10.1016/j.enggeo.2022.106585
Locat J, Demers D (1988) Viscosity, yield stress, remolded strength, and liquidity index relationships for sensitive clays. Can Geotech J 25(4):799-806. https://doi.org/10.1139/t88-088
Mbarak WK, Çinicioğlu EN, Çinicioğlu O (2020) SPT based determination of undrained shear strength: regression models and machine learning. Front Struct Civ Eng 14(1):185-198. https://doi.org/10.1007/s11709-019-0591-x
Mitchell JK, Soga K (2005) Fundamentals of Soil Behavior (Vol. 3). John Wiley and Sons, New York.
Moayedi H, Hayati S (2019) Artificial intelligence design charts for predicting friction capacity of driven pile in clay. Neural Comput Appl 31(11):7429-7445. https://doi.org/10.1007/s00521-018-3555-5
Moayedi H, Moatamediyan A, Nguyen H, et al. (2020) Prediction of ultimate bearing capacity through various novel evolutionary and neural network models. Eng Comput 36(2):671-687. https://doi.org/10.1007/s00366-019-00723-2
Saadat M, Bayat M (2022) Prediction of the unconfined compressive strength of stabilised soil by Adaptive Neuro Fuzzy Inference System (ANFIS) and Non-Linear Regression (NLR). Geomech Geoeng 17(1):80-91. https://doi.org/10.1080/17486025.2019.1699668
Sharma B, Bora PK (2003) Plastic limit, liquid limit and undrained shear strength of soil-reappraisal. J Geotech Geoenviron 129(8):774-777. https://doi.org/10.1061/(ASCE)1090-0241(2003)129:8(774)
Sharma B, Sridharan A (2018) Liquid and plastic limits of clays by cone method. Int J Geo-Eng 9(1):1-10. https://doi.org/10.1186/s40703-018-0092-0
Sherwood P, Ryley M (1970) An investigation of a cone-penetrometer method for the determination of the liquid limit. Geotechnique 20(2):203-208. https://doi.org/10.1680/geot.1970.20.2.203
Shi X, Herle I (2015) Compression and undrained shear strength of remoulded clay mixtures. Géotech Lett 5(2):62-67. https://doi.org/10.1680/geolett.14.00089
Shimobe S (2000) Correlations among liquidity index, undrained shear strength and fall cone penetration of fine-grained soils. Proceedings of Coastal Geotechnical Engineering in Practice, Balkema, Rotterdam, The Netherlands. pp 141-146.
Shimobe S, Spagnoli G (2020) Relationships between undrained shear strength, liquidity index, and water content ratio of clays. B Eng Geol Environ 79(9):4817-4828. https://doi.org/10.1007/s10064-020-01844-5
Skempton A, Northey R (1952) The sensitivity of clays. Geotechnique 3(1):30-53. https://doi.org/10.1680/geot.1952.3.1.30
Spagnoli G, Feinendegen M (2017) Relationship between measured plastic limit and plastic limit estimated from undrained shear strength, water content ratio and liquidity index. Clay Miner 52(4):509-519. https://doi.org/10.1180/claymin.2017.052.4.08
Spagnoli G, Stanjek H, Sridharan, A (2018). Some observations considering undrained shear strength, liquidity index, and fluid/solid ratio of mono-mineralic clays with water–ethanol mixtures. Can Geotech J 55(7): 1048-1053.

https://doi.org/10.1139/cgj-2017-0490
Taleb Bahmed I, Harichane K, Ghrici M, et al. (2019) Prediction of geotechnical properties of clayey soils stabilised with lime using artificial neural networks (ANNs). Int J Geotech Eng 13(2):191-203. https://doi.org/10.1080/19386362.2017.1329966
Tanaka H, Hirabayashi H, Matsuoka T, Kaneko H (2012). Use of fall cone test as measurement of shear strength for soft clay materials. Soils Found 52(4):590-599. https://doi.org/10.1016/j.sandf.2012.07.002
Terzaghi K, Peck RB, Mesri G (1996) Soil Mechanics in Engineering Practice. John Wiley and Sons, Inc., New York.
Trauner L, Dolinar B, Mišič M (2005) Relationship between the undrained shear strength, water content, and mineralogical properties of fine-grained soils. Int J Geomech 5(4):350-355. https://doi.org/10.1061/(ASCE)1532-3641(2005)5:4(350)
Ullah A, Rahman MS, Ahammad F (2017) Application of vane shear tools to asse. Res J Eng 6(1): 1-4.
Vardanega P, Haigh SK (2014) The undrained strength–liquidity index relationship. Can Geotech J 51(9):1073-1086. https://doi.org/10.1139/cgj-2013-0169
Vinod P, Sridharan A, Deepa K (2013). Remoulded shear strength at plastic and semi-solid states. Proceedings of the Institution of Civil Engineers-Geotechnical Engineering 166(4):415-424. https://doi.org/10.1680/geng.11.00071
Whyte I (1982) Soil plasticity and strength--a new approach using extrusion. Ground Eng 15(1).
Winters W (2000) Stress history and geotechnical properties of sediment from the Cape Fear diapir, Blake Ridge diapir, and Blake Ridge. Proceedings of the Ocean Drilling Program. Sci Results 164: 421-429.
Wood DM (1990) Soil Behaviour and Critical State Soil Mechanics. Cambridge University Press.
Wroth C, Wood D (1978) The correlation of index properties with some basic engineering properties of soils. Can Geotech J 15(2):137-145. https://doi.org/10.1139/t78-014
Yang S, Kvalstad T, Solheim A, Forsberg C (2006) Parameter studies of sediments in the Storegga Slide region. Geo-Mari Lett 26(4):213-224. https://doi.org/10.1007/s00367-006-0023-5
Yasun AS (2018) Capability of pocket penetrometer to evaluate unconfined compressive strength of baghdad clayey soil. Al-Nahrain J Eng Sci 21(1):66-73. https://doi.org/10.29194/NJES21010066
Yılmaz, Y, Eun, J, Panahi SS, Mousavi MS (2019) Effects of height-to-diameter ratio (H/D) for specimens with various water contents on unconfined compressive strength of a clayey soil. Eng Geol 257: 105136. https://doi.org/10.1016/j.enggeo.2019.05.013
Zadeh LA (1965) Fuzzy sets. Inf Control 8(3):338-353. https://doi.org/10.1016/S0019-9958(65)90241-X
Zentar R, Abriak NE, Dubois V (2009) Fall cone test to characterize shear strength of organic sediments. J Geotech Geoenviron 135(1):153-157. https://doi.org/10.1061/(ASCE)1090-0241(2009)135:1(153)
Zreik DA, Ladd CC, Germaine JT (1995) A new fall cone device for measuring the undrained strength of very weak cohesive soils. Geotech Test J 18(4):472-482. https://doi.org/10.1520/GTJ11022J